Dynamics Simulation and Experimental Investigation of Q-Switching in a Self-Mode-Locked Semiconductor Disk Laser

Peng Zhang, Renjiang Zhu, Tao Wang, Yadong Wu, Cunzhu Tong, Lijie Wang, and Yanrong Song

***Abstract*—Q-switching in a mode-locked laser not only makes the amplitude of every single output pulse unequal, but also limits the time width and peak power of output pulses. This paper investigates the Q-switching in a self-mode-locked semiconductor disk laser numerically and experimentally. By using the delay differential equations for passively mode-locking, conditions of Q-switching in a self-mode-locked semiconductor disk laser are numerically analyzed for the first time. Meanwhile, based on the experimental results, the causes of Q-switching tendency including the change of nonlinear refractive index and the change of soft aperture, are also discussed. Some possible measures to suppress Q-switching instability, i.e., to obtain stable continuous-wave mode-locking in a self-mode-locked semiconductor disk laser are proposed.**

***Index Terms*—Q-switching, self-mode-locking, semiconductor disk laser, delay differential equations.**

I. Introduction

OPTICALLY-pumped semiconductor disk lasers (SDLs), possess the gain superiority of semiconductor materials and geometry advantage of solid-state disk lasers. SDLs can produce good beam quality, high output power as well as tailorable oscillating wavelength simultaneously [1], [2]. Meanwhile, it is convenient for a SDL to realize mode-locking [3], [4], wavelength-tuning [5], frequency-doubling [6] or other specific operations [7].

Because of its intrinsic time characteristics of semiconductor carriers, SDLs are particularly suited for the generation of ultrashort pulses with pulse duration from picosecond to femtosecond. Since the first mode-locked SDL was reported [8], performances of such devices have been greatly improved [9], [10]. The maximum average output power has been increased to 6.4 W [11], the minimum pulse width has been decreased to 60 fs [12], and the repetition rate directly arisen from the oscillator has also been pushed to 101.2 GHz [13]. At the same time, many groups have done excellent researches on the mechanism of mode-locking in a SDL, including the effects of dispersion [14], the shaping of soliton-like pulse [15], [16], the nonequilibrium carrier dynamics and so on [17].

In addition to the above mentioned SDLs which were passively mode-locked using a semiconductor saturable absorption mirror (SESAM), researchers have found another method for mode-locking in SDLs, known as self-mode-locking (SML) [18], [19]. Some experiments of SML need to insert a slit or another Kerr medium in the laser resonator [20], [21], while other reports of SML do not need to place any additional elements [22], [23].

Currently, it is widely accepted that the SML phenomenon in a SDL originates from the Kerr effect of the semiconductor gain medium [24]. The Kerr effect can be expressed as $n = n_0 + n_2 I$, where n_0 is the refractive index without light, I is the light intensity, and n_2 is the nonlinear refractive index. It has been realized that the spatial distribution of light intensity (e.g., Gaussian distribution) will form a so-called Kerr-lens. Along with a soft or hard aperture, an equivalent saturable absorber can be produced. For SDLs, the inter-band and intra-band relaxation time of carriers are in the order of nanosecond and picosecond [25]. So, in the numerical analysis later in this paper, we would consider the Kerr effect along with an aperture in self-mode-locked SDL as a SESAM.

In view of that the carrier relaxation time in the order of nanoseconds can effectively suppress the Q-switching tendency, there is no in-depth study on the Q-switching phenomenon in mode-locked SDLs yet. However, in a passively mode-locked SDL, if the gain of laser is not sufficient, or, the modulation depth of the saturable absorber is relatively large, it will still cause undersaturation of the absorber and result in the Q-switching.

Manuscript received 12 July 2022; revised 14 August 2022; accepted 23 August 2022. Date of publication 26 August 2022; date of current version 5 September 2022. This work was supported in part by the Cooperation Project between Chongqing Local Universities and Institutions of Chinese Academy of Sciences, in part by Chongqing Municipal Education Commission under Grant HZ2021007, in part by the National Natural Science Foundation of China under Grants 61904024, 61975003, 61790584, and 62025506, in part by the Science and Technology Research Program of Chongqing Municipal Education Commission under Grant KJZD-M201900502, and in part by the State Key Laboratory of Luminescence and Applications under Grant SKLA-2019-04. *(Corresponding authors: Peng Zhang; Renjiang Zhu.)*

Peng Zhang is with the National Center for Applied Mathematics, Chongqing Normal University, Chongqing 401331, China (e-mail: zhangpeng2010@cqnu.edu.cn).

Renjiang Zhu, Tao Wang, and Yadong Wu are with the College of Physics and Electronic Engineering, Chongqing Normal University, Chongqing 401331, China (e-mail: 794243380@qq.com; 834083237@qq.com; 2065509991@qq.com).

Cunzhu Tong and Lijie Wang are with the State Key Laboratory of Luminescence and Applications, Changchun Institute of Optics, Fine Mechanics and Physics, Chinese Academy of Sciences, Changchun, Jilin 130033, China (e-mail: tongcz@ciomp.ac.cn; wanglijie@ciomp.ac.cn).

Yanrong Song is with the Faculty of Sciences, Beijing University of Technology, Beijing 100124, China (e-mail: yrsong@bjut.edu.cn).

Digital Object Identifier 10.1109/JPHOT.2022.3201986

Particularly, for a self-mode-locked SDL which is initiated by the combined action of a Kerr-lens and a soft aperture, on one hand, the change of pump intensity will lead to the change of nonlinear refractive index of gain medium. (i.e., the change of focal length of the Kerr-lens). On the other, the size of soft aperture formed by the overlap of laser and pump spot is also very sensitive to the adjustment of laser cavity. Both of them may stimulate the Q-switching tendency in a self-mode-locked SDL.

In this work, the Q-switching instability in a self-mode-locked SDL is numerically simulated using the delay differential equations for passively mode-locking. Then, according to the experimental results, the Q-switching phenomenon in a self-mode-locked SDL is further discussed and analyzed. Some possible measures for suppressing Q-switching instability, i.e., for obtaining stable continuous-wave (CW) mode-locking, are also proposed.

II. Theoretical Model and Numerical Simulations

Dynamics of mode-locking can be well explained by Haus master equations [26]. This analytical approach is widely used because of its insight into the underlying mechanism of mode-locking. However, because it's approximation of small change of the laser pulse shape within one round-trip, dynamics of some mode-locked lasers (such as fiber laser and semiconductor laser) can no longer be described satisfactorily by the master equation. Here we use another model proposed by A. G. Vladimirov et al for passively mode-locked semiconductor lasers [27], [28]. It includes a set of ordinary delay differential equations. This model avoids the approximations of small gain and loss per cavity round-trip and weak saturation, and is closer to actual condition of semiconductor laser devices.

The delay differential equations (DDEs) are expressed as:

$$\frac{1}{\gamma}\frac{\partial A}{\partial t} = \sqrt{\kappa}\exp\left\{\frac{1}{2}[(1-i\alpha_g)g(t-\tau) - (1-i\alpha_q)q(t-\tau)]\right\} \times A(t-\tau) - A(t) \quad (1)$$

$$\frac{\partial g}{\partial t} = \gamma_g(g_0 - g(t)) - \exp(-q)[\exp(g)-1]|A(t)|^2 \quad (2)$$

$$\frac{\partial q}{\partial t} = \gamma_q(q_0 - q(t)) - s[1-\exp(q)]|A(t)|^2 \quad (3)$$

where A is the electric field amplitude of laser, γ is the bandwidth of spectral filter, κ describes the total nonresonant linear intensity losses per cavity round-trip, α_g and α_q are the linewidth enhancement factors for gain medium and saturable absorber, respectively. g and q indicate the time dependent saturable gain and absorption, g_0 and q_0 denote the initial value of g and q, γ_g and γ_q are the relaxation rates in the gain and absorber, and s is the ratio of saturation energy of gain and absorber. It should be noted that the delay parameter τ equal to the cavity round-trip time, and all times in the above equations are normalized by the cavity round-trip time.

In order to compare with the experimental results later, in the numerical simulation below, we choose a linear laser cavity. The resonator is composed of a distributed Bragg reflector (DBR) at the bottom of gain chip and an external flat-concave end mirror with a radius of curvature of 150 mm. The high-reflection coated end mirror has a reflectivity of $R_1 = 99.9\%$ at laser wavelength 980 nm, and the reflectivity of DBR for laser wavelength is about $R_2 = 99\%$. In the above delay differential equations, κ is defined as the intensity transmission of output mirror, i.e., the fraction of power remaining in the cavity after each round-trip. So, we have $\kappa = \sqrt{R_1 R_2} = 0.9945$.

The active region of gain chip in our experiment is consisted of 15 InGaAs/GaAs multiple quantum wells that designed for a target emitting wavelength of 980 nm. Like reference [14], the value of gain bandwidth can be selected to be 10 nm and the corresponding bandwidth of spectral filter to be $\gamma = 200$. The cavity length used in experiment is about 140 mm, resulting in a cavity round-trip time of $\tau_r \sim 1$ ns. Considering that the typical value of gain recovery time can be chosen as 10 ns, and it should be normalized by τ_r as mentioned before, the relaxation rate of gain will be $\gamma_g = 0.1$. As for the value of g_0, it is determined through referring to the similar situation in literatures [27], [28] and [29].

Selection of the parameters of saturable absorber is a little more complicated, because there is no a real saturable absorber in a self-mode-locked SDL, but an equivalent saturable absorber composed of the Kerr-lens and the soft aperture. By using the transmission formula of light field and the split-step Fourier method, we calculate the difference of intra-cavity round-trip loss of laser with and without Kerr-lens (see Fig. 5). Then the loss difference is regarded as the modulation depth of the equivalent saturable absorber, and parameter q_0 in the delay differential equations is determined.

It can be said that SML in a SDL depends on the equivalent saturable absorber, which relies on the Kerr-lens, i.e., the nonlinear refractive index. Since the nonlinear refractive index n_2 in semiconductor gain medium is caused by carrier density, and the typical value of recovery time of carrier is about 10 ps. Therefore, the recovery time of the equivalent saturable absorber is chosen to be 10 ps. After normalized by the cavity round-trip time of 1 ns, the value of relaxation rate in absorber is $\gamma_q = 100$.

Parameter s is defined as $s = E_{sat,g}/E_{sat,q}$, and the saturation energy of gain is selected to be $E_{sat,g} = 50$ nJ (corresponding to 100 μm spot radius) [14]. Considering that the equivalent saturable absorber is consisted of the Kerr-lens and a soft aperture, the parameter $E_{sat,q}$ in this paper is estimated using the critical power of Kerr effect, which can be expressed as [30], [31]

$$P_{cr} = \frac{\pi(0.61)^2\lambda^2}{8n_0 n_2} \quad (4)$$

For $\lambda = 980$ nm, $n_0 = 3.5$, $n_2 = 1\times10^{-16}$ m^2/W [32], [33], and pulse width of 5 ps, the above P_{cr} corresponds to a saturation energy of about 2 nJ, so the estimated value of the saturation parameter is $s = 25$.

All parameters used in the simulations below are summarized and listed in Table I. Linewidth enhancement factors for gain medium and saturable absorber are not included in this work. The parameter g_0 will increase with increased pump intensity. q_0 will also change with the various pump intensity, because pump intensity can change the nonlinear refractive index of gain

TABLE I
PARAMETERS USED IN THE SIMULATIONS

γ	κ	γ_g	γ_q	g_0	q_0	s	α_g	α_q
200	0.9945	0.1	100	1.8-2.6	0.5-1.5	25	0	0

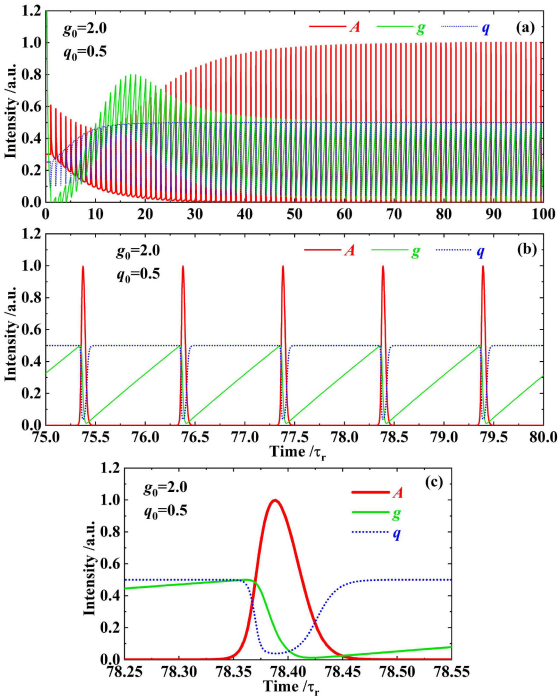

Fig. 1. Simulated evolution of the self-mode-locked pulses using DDEs. (a) Contains 100 intracavity cycles, (b) is an enlargement of (a), and (c) Clearly shows the process of pulse formation of a single pulse.

medium, thus change the focal length of Kerr-lens and have an influence on the value of q_0. In addition, q_0 will be obviously affected by the radium of soft aperture. Except g_0 and q_0, other parameters remain a fixed value in the numerical simulation.

We numerically solve equations (1)–(3) using the famous Runge-Kutta method. Fig. 1 shows the time-dependent field amplitude A, gain g and absorption q when g_0 and q_0 are chosen to be 2.0 and 0.5, respectively. Because the time has been normalized by the cavity round-trip time τ_r in the equations, the unit of time axis in figure is τ_r. We can see in Fig. 1(a)(containing 100 intracavity cycles) that the pulse becomes steady and reaches a stable CW mode-locking after about 60 round-trips. Fig. 1(b) is an enlargement of Fig. 1(a). Fig. 1(c) clearly shows the process of pulse formation. At a certain time, the absorption of the absorber begins to decline due to saturation. When the absorption drops below the gain, the net gain window opens and the pulse shape begins. Then the gain also gradually tends to saturation and begins to decrease. Once the gain is equal to the absorption, the amplitude of the pulse reaches the maximum value. This is followed by the respective recovery of absorber and gain medium, as well as the similar formation process of the next pulse.

According to the research results reported by C. Honninger et al, the stability condition against Q-switching in a passively mode-locked laser can be express as [34]

$$E_p^2 > E_{sat,g} E_{sat,q} \Delta R \tag{5}$$

where E_p is pulse energy and ΔR is modulation depth. Obviously, for given $E_{sat,g}$ and $E_{sat,q}$, excessive ΔR or relatively small E_p will trigger unwanted Q-switching.

For SML described by equations (1)–(3), the influence of g_0 on Q-switching instability is similar to that of $E_{sat,g}$, and the effect of q_0 is same as that of ΔR. Fig. 2 shows the calculated pulse evolution in a self-mode-locked SDL with $q_0 = 1.5$ and various g_0 from 1.8 to 2.6. The insets in the upper left corner are the calculation results on a larger time scale, which can show whether the pulse reaches a stable state more accurately.

As can be seen from Fig. 2(a), the pulse reaches a stable Q-switched mode-locking after about 500 round-trips, and the period of Q-switching envelope is about 55 τ_r. In Fig. 2(b), the time required to reach stable Q-switched mode-locking is shorter (about 150 round-trips), and the period of Q-switching envelope is shorter too (about 40 τ_r). It takes about 100 and 50 round-trips to come to steady Q-switching in Fig. 2(c) and (d), respectively. In general, from (a) to (d), with the gradually increased g_0, the time required for establishing stable Q-switched mode-locking becomes shorter and shorter, and the depth of Q-switching envelope turns smaller and smaller. In other word, the Q-switching gradually disappears with increased g_0. In Fig. 2(e), we can see that about 80 intracavity round-trips later, the pulses have developed into an ideal CW mode-locked pulse train.

Fig. 2(f) shows the time-dependent A, g and q when the g_0 and q_0 are 1.8 and 1.5, respectively. As shown in Fig. 2(f), Q-switching is originated from the undersaturation of the absorber in the development of mode-locking. When the absorber is partially saturated, the gain begins to saturate immediately after it. Then, the net gain window is formed and the pulse is established. However, the amplitude of the net gain window is small at this time, and the corresponding pulse intensity is not big. As pump continuing, the peak value of established pulse will be higher and higher. Only when the absorber is fully saturated, the amplitude of net gain window reaches the maximum value and the pulse peak gets the highest magnitude. The time required for absorber from partial saturation to full saturation determines the time width of Q-switching, which obviously decreases with increased g_0. It is also clear that the undersaturation of absorber is resulted from the relatively small g_0, or relatively weak pumping intensity. This has been fully illustrated by the fact that the Q-switching in Fig. 2(a)–(e) gradually disappears with increased g_0.

In the DDE model, g and q describe the saturable gain and loss in the cavity, respectively, and κ describes the total nonresonant linear intensity loss in a round-trip. Thus, the threshold condition for lasing is given by $g = q - \ln(\kappa)$. We plot the calculated Q-switching, the CW mode-locking and the lasing thresholds with various (q_0, g_0) and fixed (κ, γ, γ_g, γ_q, s) in Fig. 3. It can be concluded from Fig. 3 that for a self-mode-locked SDL using Kerr effect, Q-switching will exist in a certain range between

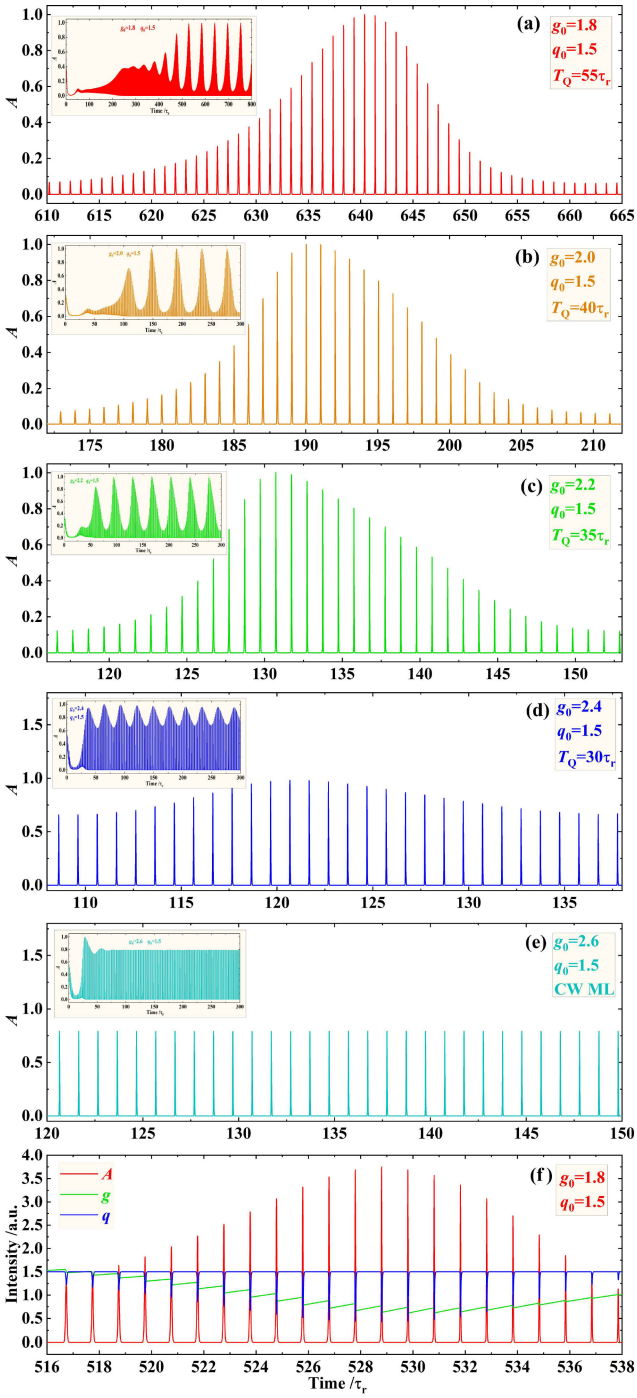

Fig. 2. Calculated pulse train of SML in a SDL under $q_0 = 1.5$ and various value of g_0. (a) $g_0 = 1.8$, (b) $g_0 = 2.0$, (c) $g_0 = 2.2$, (d) $g_0 = 2.4$, (e) $g_0 = 2.6$. The insets in the upper left corner show the calculation results on a larger time scale.

the CW operation and CW mode-locking. For a given g_0, larger the q_0 is, wider the Q-switching region will be.

III. Experimental Results and Discussions

The gain chip used in experiment is epitaxially grown in reverse sequences as: the AlGaAs etch stop layer with high Al composition, the GaAs protect layer, the AlGaAs window layer with high barrier, the active region, the DBR and the antioxidant GaAs cap layer. There are 15 InGaAs/GaAsP quantum wells in the active region. The content of In in InGaAs well layer is designed to meet the target laser wavelength of 980 nm, and the content of P in GaAsP barrier layer must be adequate to compensate the strain but not too much to absorb the pumping energy. The DBR is composed of 30 pairs alternate AlGaAs layers with high Al and low Al composition, and the designed center wavelength and high-reflectivity bandwidth of it are 980 nm and 100 nm respectively. According to the test data given by manufacturer, the reflectivity of DBR at 980 nm wavelength is about $R_2 = 99\%$.

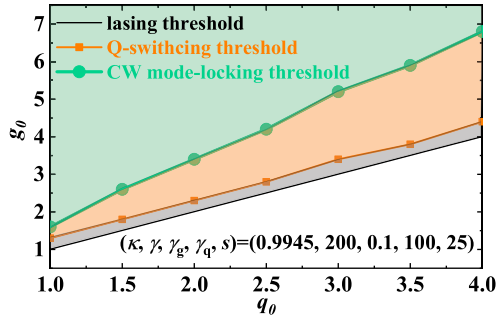

Fig. 3. Computed Q-switching threshold, CW mode-locking threshold and the lasing threshold with various (q_0, g_0) and fixed (κ, γ, γ_g, γ_q, s).

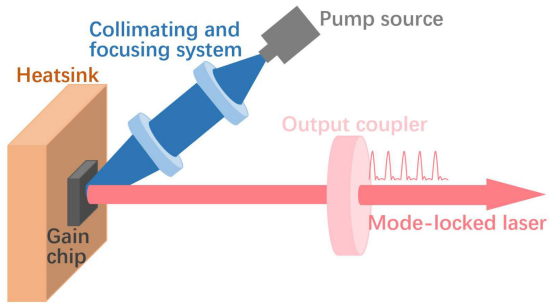

Fig. 4. Experimental diagram of the self-mode-locked SDL.

When the grown wafer is split to small chips with 4 mm×4 mm dimension, the epitaxial end face is metalized with titanium-platinum-aurum sequentially. Then the chip is bonded to a copper heatsink, and the substrate is removed using chemical etch. A high-reflectivity coated (for 980 nm wavelength) plane-concave mirror with 150 mm curvature radius is employed as the end mirror to form a linear cavity, and the reflectivity of the end mirror at 980 nm wavelength is $R_1 = 99.9\%$. The pump source is a 808 nm fiber-coupled semiconductor diode laser with 30 W output power, and the core diameter of its pigtail fiber is 200 μm. Fig. 4 shows the experimental diagram.

SML can be achieved by introducing a saturable absorber, which is formed by the combination of the Kerr medium plus a soft aperture. In experiment, two key conditions are required to start the SML. Firstly, the intracavity light with high enough circulating power is needed to ensure that there are desired

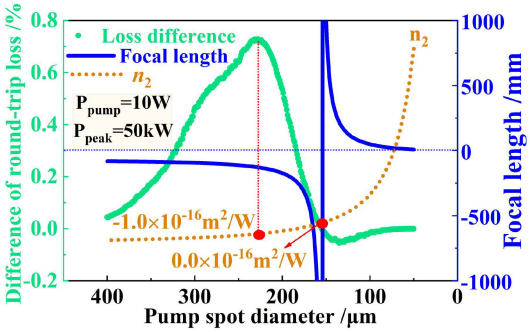

Fig. 5. Calculated nonlinear refractive index n_2 of gain medium, focal length f of Kerr-lens, and the difference of round-trip loss with and without Kerr-lens under various pump spot size. The pump power and the peak power of the noise pulse are supposed to be 10 W and 50 kW, respectively. The nonlinear reflective index n_2 is obtained from reference [32].

noises with high enough peak power to generate the primary Kerr effect. Secondly, an aperture with appropriate size is necessary to provide a certain difference between the cavity loss of mode-locking and continuous operation, so to initiate and stabilize mode-locking. Among them, the enhancement of intracavity circulating optical power can be easily realized by increasing the pump intensity. In practice, more care should be taken to choose an aperture with proper size.

In order to estimate the appropriate size of soft aperture, we firstly calculated the nonlinear refractive index n_2 of gain medium under different pump spot sizes (keeping the pump power a constant). Data of nonlinear refractive index n_2 under various pump power density provided by reference [32] are used in the calculation, and the simulated results are shown by yellow dotted line in Fig. 5. Then, the focal length of Kerr-lens is carried out based on the formula

$$f = \frac{\omega^2}{4\pi n_2 I_p L} \tag{6}$$

where ω is the radium of light spot, I_p is the peak light intensity, and L is the length of Kerr medium. The calculated focal length f of Kerr-lens can be seen from the blue solid line in Fig. 5. Finally, by using the split-step Fourier method, the amplitude of the light field is computed when it completes a round-trip in the cavity, and the difference of the round-trip loss experienced by the laser beam with and without Kerr-lens is carried out, as shown by the green solid line in Fig. 5. In the calculation, the length of Kerr medium is equal to the thickness of active region in gain chip, the pump power is set to be 10 W, and the value of pulse peak power is 50 kW. As mentioned before, the transmittance of output coupler is 99.9%. Supposing a pulse width of 5 ps and a pulse repetition rate of 1 GHz, the above 50 kW peak power corresponds to an intracavity circulating power of 250 W and an output power of 250 mW, which is roughly consistent with the reality of our experiment.

Obviously, a smaller pump spot is favorable for a focused beam because it will introduce more loss to an ordinary beam and provide larger difference between the intracavity loss with and without Kerr-lens. However, a smaller pump spot also means a higher pump power density. When the pump power density is increased, n_2 will change from negative to positive, and its absolute value will firstly decrease and then increase [32]. This will result in a corresponding change of the focal length of Kerr-lens. So, as shown in Fig. 5 that the difference of round-trip loss with and without Kerr-lens has a peak value when the pump spot diameter is about 220 μm, whose pump density corresponds to a n_2 about -1.0×10^{-16} m^2/W. Further reducing of the pump spot will lead to a gradual decrease of the loss difference.

In our experiment, the cavity length is set to be about 140 mm, corresponding to a 240 μm diameter laser spot on gain chip. To achieve better transverse mode and stability of mode-locking, the laser cavity can be adjusted slightly around 140 mm. We use a 1:1.3 imagine lens pair to collimate and focus the pump beam on gain chip, and the pump spot size can be finely tuned by slightly changing the imagine distance. The soft aperture is formed by the overlap of pump and laser spot on gain chip. A Thorlabs DET08C InGaAs Biased Detector (with 5 GHz bandwidth, 70 ps rise time, 110 ps fall time, and 800–1700 nmw wavelength range) is used to receive the mode-locked pulse train, and the signal is then sent to a Tektronix MSO68B 6 Series Mixed Signal Oscilloscope (with 10 GHz bandwidth and 50 Gs/s sampling rate) for observation. The electric signal is also sent to a Rigol DSA875 spectrum analyzer (with 7.5 GHz bandwidth and 100 Hz–1 MHz resolution bandwidth) to record the repetition rate of pulse train. The time width of the mode-locked pulse is measured using a Femtochrome FR-103XL autocorrelator (with $>$4 Hz repetition rate, $>$175 ps scan range and $<$5 fs resolution ratio), and the laser spectrum is obtained from an Ocean Optics MAYA2000PRO-NIR spectrometer (with 780–1180 nm wavelength range and 0.18 nm resolution ratio).

It has been found that the pump threshold of laser is about 0.522 W. When the pump power is increased to 1.036 W, we have the Q-switched mode-locking in the laser, and the output pulse train is show in Fig. 6(a). The period of Q-switching envelope decreases from 27 ns in Fig. 6(a) to 9 ns in Fig. 6(b) when the pump power is increased from 1.036 to 2.000 W. Stable CW mode-locking can be produced when the pump power reaches 2.126 W, as shown in Fig. 6(c). It can be concluded that with higher pump power, the period of Q-switching envelope becomes smaller, until it finally transitions to the ideal CW mode-locking, and this is consistent with the previous numerical analysis.

A close view of the pulse train in Fig. 6(b) is redrawn in Fig. 7(a), and its corresponding radio frequency (RF) spectrum is shown in Fig. 7(b). The periods of Q-switching and mode-locking in Fig. 7(a) are approximately $T_Q = 9$ ns and $T_{ML} = 1$ ns, and their corresponding RF spectrum are $f_Q = 0.11$ GHz and $f_{ML} = 1.03$ GHz, respectively. f_Q is mainly affected by pumping intensity, while f_{ML} is only determined by cavity length.

In Fig. 7(b), the first signal $f_Q = 0.11$ GHz is obviously arisen from the period of envelope of Q-switching, which is about 9 ns. The third signal $f_{ML} = 1.03$ GHz certainly corresponds to the period of mode-locked pulse train and is in coordination with 145 mm cavity length. For the signals on the left and right sides of f_{ML}, the frequency intervals between them and f_{ML} are strictly equal to f_Q. So, it can be concluded that they are the difference-frequency and sum-frequency signals of f_{ML}

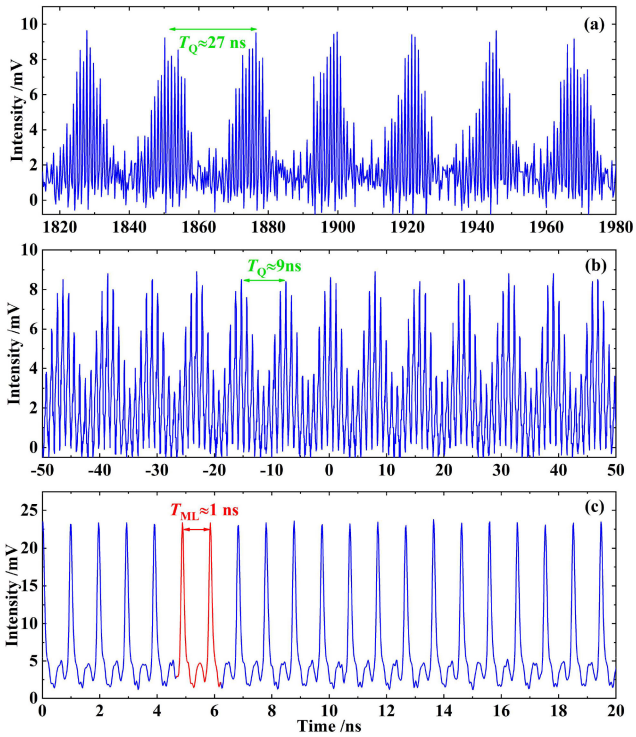

Fig. 6. Q-switching (a), (b) and CW mode-locking (c) in a self-mode-locked SDL under different pump power.

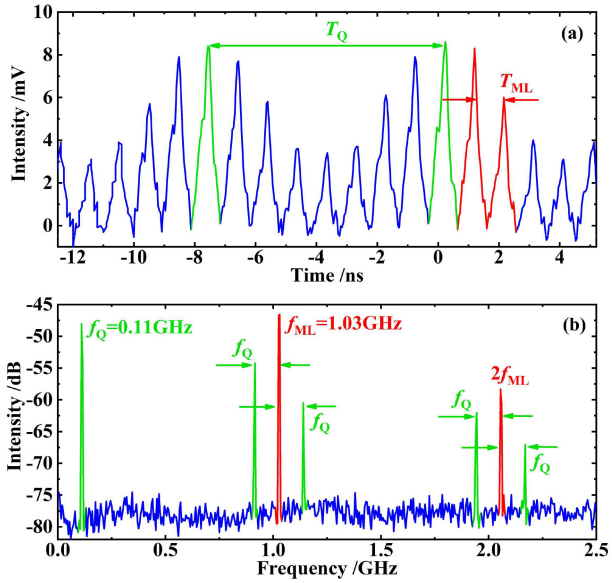

Fig. 7. Close view of the pulse train with 9 ns envelope period of Q-switched mode-locking (a), and its corresponding RF spectrum (b). The sum-frequency signals and difference-frequency signals between f_{ML} and f_Q, as well as $2f_{ML}$ and f_Q are also shown.

and f_Q. Fig. 7(b) also shows the second harmonic of f_{ML}, and the difference-frequency and sum-frequency signals of $2f_{ML}$ and f_Q. It should be noted that reference [35] mentioned a RF spectrum similar as in Fig. 7(b). However, the authors believed

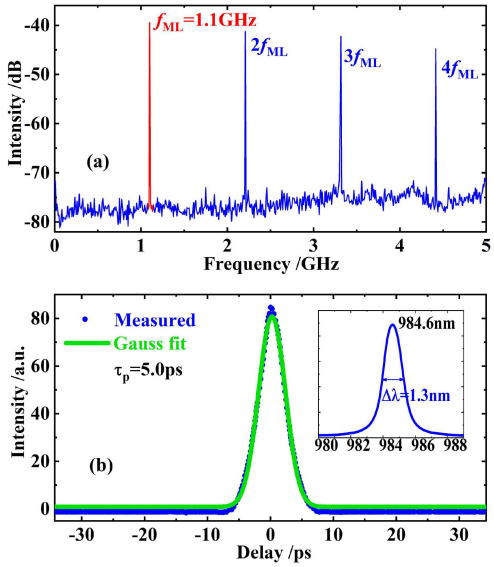

Fig. 8. RF spectra (a) and autocorrelation measurement (b) of the CW mode-locked pulse train with 20 °C temperature and 5 W pump power. The fundamental frequency as well as its higher harmonics are also shown in (a), and the inset at the right side in (b) is the corresponding laser spectrum.

that those subpeaks beside f_{ML} and $2f_{ML}$ should be attributed to the frequency spacing of transverse modes.

Slowly increasing the pump power and slightly adjusting the cavity length and pump spot size can weaken the Q-switching gradually and make it disappear at last. That is, the laser will transit to a stable CW mode-locking state as described before. Fig. 8 shows the RF spectrum and autocorrelation measurement of the CW mode-locked pulse train with 20 °C temperature and 5 W pump power. In Fig. 8(a), the frequency spectrum of Q-switched signal f_Q and its difference- and sum-frequency signals with mode-locked signal f_{ML} are completely disappeared. The amplitude of f_{ML} is also significantly increased with a signal-to-noise ratio exceeding 40 dB, indicating an ideal CW mode-locking. The fundamental frequency of 1.1 GHz in Fig. 8(a) corresponds a cavity length about 140 mm, and higher harmonics up to fourth harmonics are also shown.

As can be seen from the autocorrelation trace of the output pulses in Fig. 8(b), the duration of mode-locked pulse is about 5.0 ps by using Gaussian fit. Along with the 1.3 nm spectral width of laser shown in the right side, it can be estimated that the time-bandwidth product of CW mode-locked pulse is approximately 1.5, over three times of 0.441 (the value of Fourier-transform-limited Gaussian pulse). This means an obvious frequency chirp is included in laser pulse. Since there are no other elements that could cause the frequency chirp in the laser cavity, the above frequency chirp clearly comes from the semiconductor gain medium. It should be noted that in a semiconductor gain medium, Kerr effect exists in both spatial and temporal domains. Kerr effect caused by the spatial distribution of light intensity (e.g., Gaussian distribution) will form a so-called Kerr-lens, and can start the self-mode-locking. On the other hand, the Kerr effect caused by a time-varying light intensity $I(t)$ of pulse will result in a time-varying nonlinear refractive index $n(t) = n_0 + n_2 I(t)$. This time-varying nonlinear

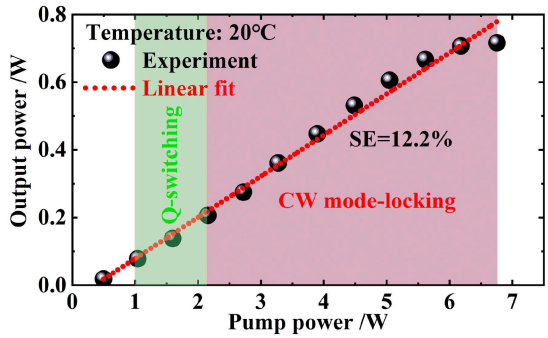

Fig. 9. Output powers versus pump powers under 20 °C temperature.

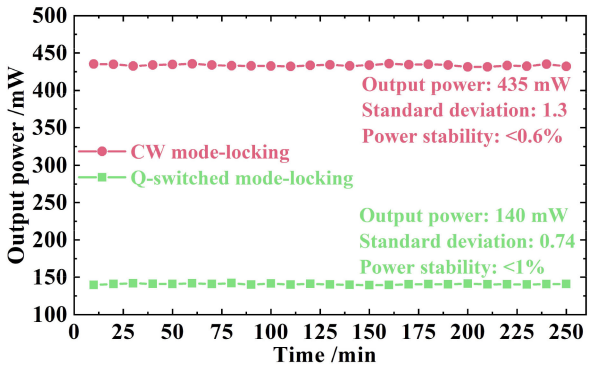

Fig. 10. Power stabilities of the SML SDL under CW and Q-switched mode-locking.

refractive index will change the phase of pulse and produce new frequency components, thus generate frequency chirp.

With condition of 20 °C temperature and about 220 μm pump spot diameter, output powers of the self-mode-locked laser under various pump powers are shown in Fig. 9. It can be seen from Fig. 9 that the lasing threshold, the Q-switching threshold, and the CW mode-locking threshold are 0.522 W, 1.036 W and 2.126 W, respectively. The output power increases almost linearly with the risen pump power, until it begins to decrease when the pump power is beyond 6.755 W. The linear fit shows a slope efficiency (SE) of about 12.2% of the laser, while the maximum output power is 0.716 W, and the maximum optical-to-optical efficiency is about 11.4%.

Fig. 10 shows the stabilities of output power under CW (435 mW) and Q-switched (140 mW) mode-locking. The values of output power are recorded every 10 minutes, and the measurement time is 4 hours. It can be seen from Fig. 9 that for both CW and Q-switch mode-locking, the values of standard deviation are relatively small, and the stabilities of output power are also relatively satisfactory.

IV. Conclusion

In summary, we have investigated the Q-switching in a self-mode-locked SDL numerically and experimentally. By solving the DDEs for passively mode-locking, it has been found that the undersaturation of saturable absorber is the direct cause of Q-switching. More specifically, relatively large modulation depth of saturable absorber or relatively small pump intensity are the main reasons for Q-switching in a self-mode-locked SDL. The period and the depth of Q-switching envelope will decrease with increased pump intensity until the laser finally transitions to CW mode-locking. In the theoretical calculation, on one hand, a smaller pump spot is favorable for a focused beam because it will introduce more loss to an ordinary beam and provide larger difference between the intracavity loss with and without Kerr-lens. On the other, a smaller pump spot also means a higher pump power density and will result in a corresponding change of the focal length of Kerr-lens. So, the difference of round-trip loss with and without Kerr-lens has a peak value. A proper pump spot with diameter neither too large nor too small should be selected carefully to start the mode-locking. We have experimentally verified the above conclusions, and the achieved self-mode-locked laser has a maximum output power of 0.716 W and a slope efficiency of about 12.2%

References

[1] M. Kuznetsov, F. Hakimi, R. Sprague, and A. Mooradian, "High-power (>0.5-W CW) diode-pumped vertical-external-cavity surface-emitting semiconductor lasers with circular TEM_{00} beams," *IEEE Photon. Technol. Lett.*, vol. 9, no. 8, pp. 1063–1065, Aug. 1997.

[2] M. Guina, A. Rantamäki, and A. Härkönen, "Optically pumped VECSELs: Review of technology and progress," *J. Phys. D Appl. Phys.*, vol. 50, no. 38, Aug. 2017, Art. no. 383001.

[3] U. Keller and A. C. Tropper, "Passively mode-locked surface-emitting semiconductor lasers," *Phys. Rep.*, vol. 429, no. 2, pp. 67–120, Jun. 2006.

[4] J. T. Meyer, M. L. Lukowski, C. Hessenius, E. M. Wright, and M. Fallahi, "High peak power, sub-ps green emission in a passively mode locked W-cavity VECSEL," *Opt. Exp.*, vol. 28, no. 4, pp. 5794–5800, Feb. 2020.

[5] A. Broda, A. Wójcik-Jedlińska, I. Sankowska, M. Wasiak, M. Wieckowska, and J. Muszalski, "A 95-nm-wide tunable two-mode vertical external cavity surface-emitting laser," *IEEE Photon. Technol. Lett.*, vol. 29, no. 24, pp. 2215–2218, Dec. 2017.

[6] M. Fallahi et al., "5-W yellow laser by intracavity frequency doubling of high-power vertical-external-cavity surface-emitting laser," *IEEE Photon. Technol. Lett.*, vol. 20, no. 20, pp. 1700–1702, Oct. 2008.

[7] A. Rahimi-Iman, "Recent advances in VECSELs," *J. Opt.-U.K.*, vol. 18, no. 9, Aug. 2016, Art. no. 093003.

[8] S. Hoogland et al., "Passively mode-locked diode-pumped surface-emitting semiconductor laser," *IEEE Photon. Technol. Lett.*, vol. 12, no. 9, pp. 1135–1137, Sep. 2000.

[9] B. W. Tilma et al., "Recent advances in ultrafast semiconductor disk lasers," *Light Sci. Appl.*, vol. 4, no. 7, Jul. 2015, Art. no. e310.

[10] M. A. Gaafar, A. Rahimi-Iman, K. A. Fedorova, W. Stolz, E. U. Rafailov, and M. Koch, "Mode-locked semiconductor disk lasers," *Adv. Opt. Photon.*, vol. 8, no. 3, pp. 370–400, Sep. 2016.

[11] B. Rudin et al., "High-power MIXSEL: An integrated ultrafast semiconductor laser with 6.4 W average power," *Opt. Exp.*, vol. 18, no. 26, pp. 27582–27588, Dec. 2010.

[12] A. H. Quarterman et al., "A passively mode-locked external-cavity semiconductor laser emitting 60-fs pulses," *Nat. Photon.*, vol. 3, no. 12, pp. 729–731, 2009.

[13] M. Mangold, C. A. Zaugg, S. M. Link, M. Golling, B. W. Tilma, and U. Keller, "Pulse repetition rate scaling from 5 to 100 GHz with a high-power semiconductor disk laser," *Opt. Exp.*, vol. 22, no. 5, pp. 6099–6107, Mar. 2014.

[14] R. Paschotta, R. Häring, A. Garnache, S. Hoogland, A. C. Tropper, and U. Keller, "Soliton-like pulse-shaping mechanism in passively mode-locked surface-emitting semiconductor lasers," *Appl. Phys. B*, vol. 75, no. 4, pp. 445–451, Sep. 2002.

[15] A. Garnache, S. Hoogland, A. C. Tropper, I. Sagnes, G. Saint-Girons, and J. S.Roberts, "Sub-500-fs soliton-like pulse in a passively mode-locked broadband surface-emitting laser with 100 mW average power," *Appl. Phys. Lett.*, vol. 80, no. 21, pp. 3892–3894, May 2002.

[16] B. G. Bale, S. Boscolo, and S. K. Turitsyn, "Dissipative dispersion-managed solitons in mode-locked lasers," *Opt. Lett.*, vol. 34, no. 21, pp. 3286–3288, Nov. 2009.
[17] I. Kilen, J. Hader, J. V. Moloney, and S. W. Koch, "Ultrafast nonequilibrium carrier dynamics in semiconductor laser mode locking," *Optica*, vol. 1, no. 4, pp. 192–197, Oct. 2014.
[18] L. Kornaszewski, G. Maker, G. P. Malcolm, M. Butkus, E. U. Rafailov, and C. J. Hamilton, "SESAM-free mode-locked semiconductor disk laser," *Laser Photon. Rev.*, vol. 6, no. 6, pp. L20–L23, 2012.
[19] M. Gaafar et al., "Self-mode-locking semiconductor disk laser," *Opt. Exp.*, vol. 22, no. 23, pp. 28390–28399, Nov. 2014.
[20] M. Gaafar et al., "Harmonic self-mode-locking of optically pumped semiconductor disc laser," *Electron. Lett.*, vol. 50, no. 7, pp. 542–543, Mar. 2014.
[21] J. V. Moloney, I. Kilen, A. Baumner, M. Scheller, and S. W. Koch, "Nonequilibrium and thermal effects in mode-locked VECSELS," *Opt. Exp.*, vol. 22, no. 6, pp. 6422–6427, Mar. 2014.
[22] R. Bek et al., "Self-mode-locked AlGaInP-VECSEL," *Appl. Phys. Lett.*, vol. 111, no. 18, 2017, Art. no. 182105.
[23] C. H. Tsou, H. C. Liang, K. F. Huang, and Y. F. Chen, "Observation of reflection feedback induced the formation of bright-dark pulse pairs in an optically pumped semiconductor laser," *Opt. Exp.*, vol. 24, no. 12, pp. 13000–13008, Jun. 2016.
[24] C. Kriso et al., "Microcavity-enhanced Kerr nonlinearity in a vertical-external-cavity surface-emitting laser," *Opt. Exp.*, vol. 27, no. 9, pp. 11914–11929, 2019.
[25] U. Keller et al., "Semiconductor saturable absorber mirrors (SESAM's) for femtosecond to nanosecond pulse generation in solid-state lasers," *IEEE J. Sel. Topics Quantum Electron.*, vol. 2, no. 3, pp. 435–453, Sep. 1996.
[26] H. A. Haus, "Mode-locking of lasers," *IEEE J. Sel. Topics Quantum Electron.*, vol. 6, no. 6, pp. 1173–1185, Nov./Dec. 2000.
[27] A. G. Vladimirov, D. Turaev, and G. Kozyreff, "Delay differential equations for mode-locked semiconductor lasers," *Opt. Lett.*, vol. 29, no. 11, pp. 1221–1223, Jun. 2004.
[28] A. G. Vladimirov and D. Turaev, "Model for passive mode locking in semiconductor lasers," *Phys. Rev. A*, vol. 72, no. 3, Sep. 2005, Art. no. 033808.
[29] R. Arkhipov et al., "Hybrid mode locking in semiconductor lasers: Simulations, analysis, and experiments," *IEEE J. Sel. Topics Quantum Electron.*, vol. 19, no. 4, Jul./Aug. 2012, Art. no. 1100208.
[30] D. Huang, M. Ulman, L. H. Acioli, H. A. Haus, and J. G. Fujimoto, "Self-focusing-induced saturable loss for laser mode locking," *Opt. Lett.*, vol. 17, no. 7, pp. 511–513, Apr. 1992.
[31] T. Brabec, C. Spielmann, P. F. Curley, and F. Krausz, "Kerr lens mode locking," *Opt. Lett.*, vol. 17, no. 18, pp. 1292–1294, Sep. 1992.
[32] A. H. Quarterman, M. A. Tyrk, and K. G. Wilcox, "Z-scan measurements of the nonlinear refractive index of a pumped semiconductor disk laser gain medium," *Appl. Phys. Lett.*, vol. 106, no. 1, Jan. 2015, Art. no. 011105.
[33] C. Kriso et al., "Probing the ultrafast gain and refractive index dynamics of a VECSEL," *Appl. Phys. Lett.*, vol. 119, no. 19, Feb. 2021, Art. no. 191105.
[34] C. Hönninger, R. Paschotta, F. Morier-Genoud, M. Moser, and U. Keller, "Q-switching stability limits of continuous-wave passive mode locking," *J. Opt. Soc. Amer. B*, vol. 16, no. 1, pp. 46–56, Jan. 1999.
[35] H. C. Liang, C. H. Tsou, Y. C. Lee, K. F. Huang, and Y. F. Chen, "Observation of self-mode-locking assisted by high-order transverse modes in optically pumped semiconductor lasers," *Laser Phys. Lett.*, vol. 11, no. 10, Sep. 2014, Art. no. 105803.